ISCRA-2021

Studies of heliospheric modulation of cosmic rays at ShICRA SB RAS and prospects of their further development

P.Yu. Gololobov, S.A. Starodubtsev, G.F. Krymsky, S.I. Petukhov, V.G. Grigoryev, I.S. Petukhov, A.S. Petukhova, S.K. Gerasimova, S.N. Taneev, V.I. Kozlov, A.S. Zverev

Moscow, 2021

Structure

1. Modern statement of Yakutsk CR spectrograph after A.I. Kuzmin
2. Metodology of treatment of data of ground-based CR detectors
3. Results of investigation of various aspects of CR heliospheric modulation performing in ShICRA SB RAS :
    1. Basic model of heliospheric modulation of CRs
    2. Theory of accelerations of SCR (SEP);
    3. Theory of formation of FD in magnetic clouds;
    4. The structure of the heliosphere (north-south asymmetry);
    5. Tensor anisotropy of CRs;
    6. Application of CRs in forecasting of Space Weather

1. Modern statement of Yakutsk CR spectrograph after A.I. Kuzmin

Figure. Photo of A.I. Kuzmin (1922 — 1996) showing to the colleagues a plan of CR spectrograph. In 2009 the spectrograph will be named after him.

1. Modern statement of Yakutsk CR spectrograph after A.I. Kuzmin

Location: **$61^\circ 59'$ N $129^\circ 41'$ E** Vertical cutoff rigidity Rc=**1.65 GV** Detection energy range: **2-300 GeV**

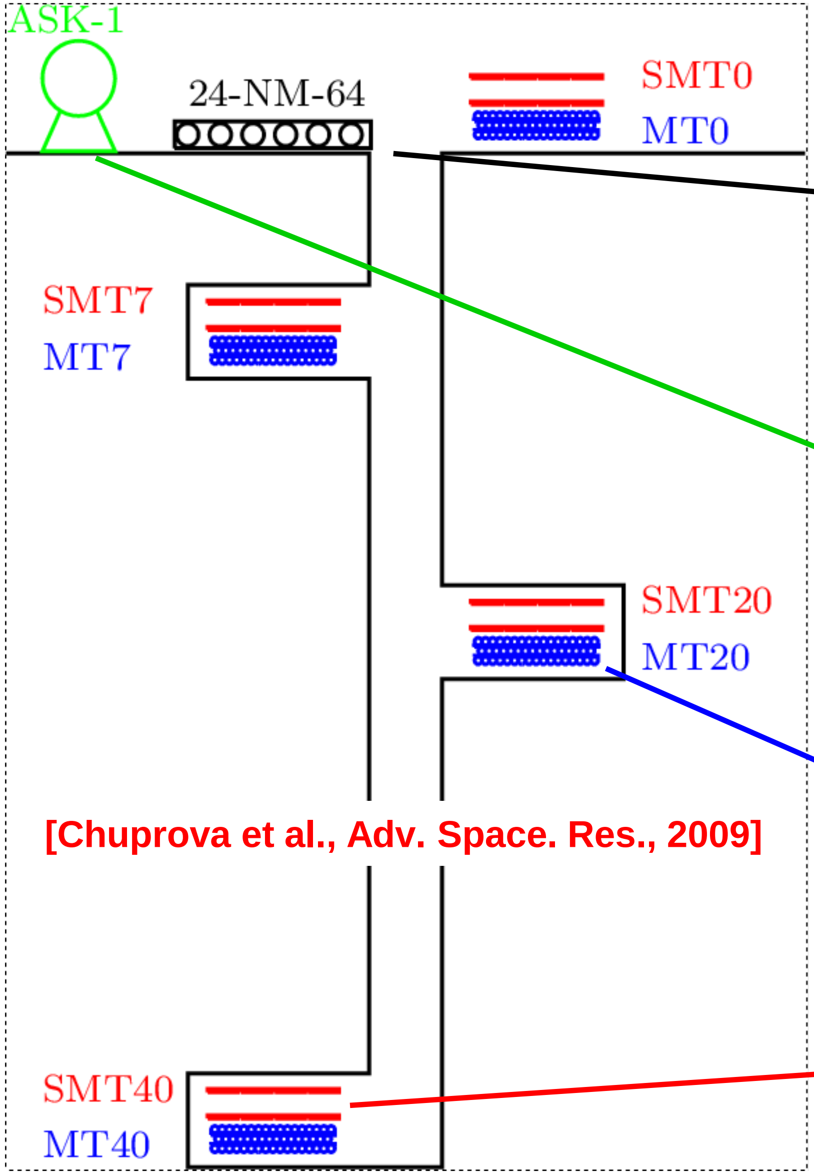

[Chuprova et al., Adv. Space. Res., 2009]

24-NM-64 – Standart NM detectors based on gas-discharge counters SNM-15. Operates since 1957. www.ysn.ru/ipm

ASK-1. a spherical ionization chamber of 950 liters in volume, filled with a chemically pure argon (99.5%) up to pressure 10,2 atм. Operates during 1953-2003. Was restored in 2019. https://www.ysn.ru/ipm/ASK-1/

MT - Muon telescope based on proportional counters SGM-14. Operates since 1972-nowadays. Effective detection area 2×1.3 m^2 . 5 independent direction of registration www.ysn.ru/ipm

SMT - Muon telescope based on scintillation detectors SC-301. Operates since 2011. Effective detection area $2{\times}4$ m^2. 13 independent direction of registration. www.ysn.ru/smt

1. Modern statement of Yakutsk CR spectrograph after A.I. Kuzmin

Level	0 m w.e.	7 m w.e.	20 m w.e.	40 m w.e.
MT based on SGM-14	1.16×10^6	0.54×10^6	0.26×10^6	0.11×10^6
MT based on SC-301	1.47×10^6	0.68×10^6	0.33×10^6	0.12×10^6

Table. Comparison of count rates of SMT and MT

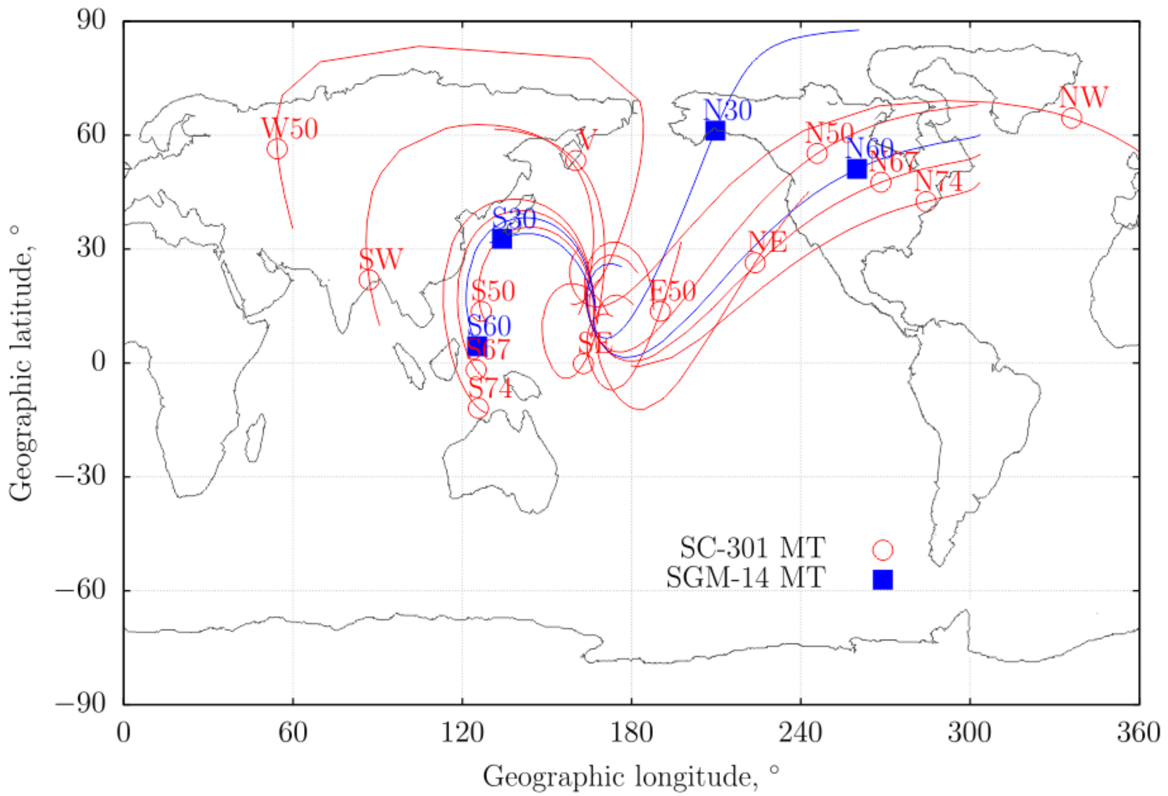

Fig. Asymptotic viewing directions of Yakutsk MTs based on SGM-14 (red) and SC-301 (black). The points corresponds to median energies of the MT directions.

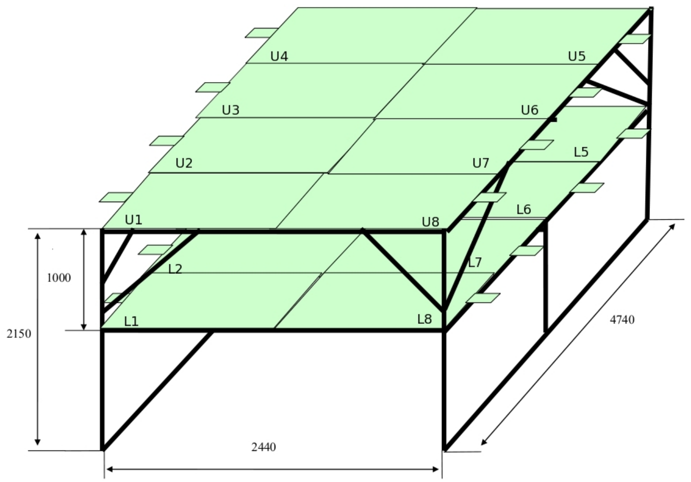

Fig. Principal scheme of SMT construction
[Gerasimova et al., Inst. Exp. Tech., 2021]

MT vs SMT

- Better angular resolution (13 independent directions for SMT vs 5 for MT)
- Narrower receiving cone
- Better statistical accuracy

2. Metodology of treatment of data of ground-based CR detectors

Computations of CR trajectories in the geomagnetic field
[Dorman, Smirnov, Tyasto, 1971]

Method of coupling coefficients (receiving vectors)
[Dorman, 1957]

Method of receiving vectors [Krymsky et al., Geomag. Aeron, 1966, 1967] *(in Russian)*

$$I(\theta,\phi)=\sum_{n=0}^{\infty}\sum_{m=0}^{\infty}(a_n^m\cos m\phi+b_n^m\sin m\phi)P_n^m(\sin\theta)\qquad \vec{A}=(a_n^m,b_n^m)\qquad R=(x_n^m,y_n^m)\qquad 0\le m\le n<\infty,\qquad I=\vec{A}\cdot\vec{R},$$

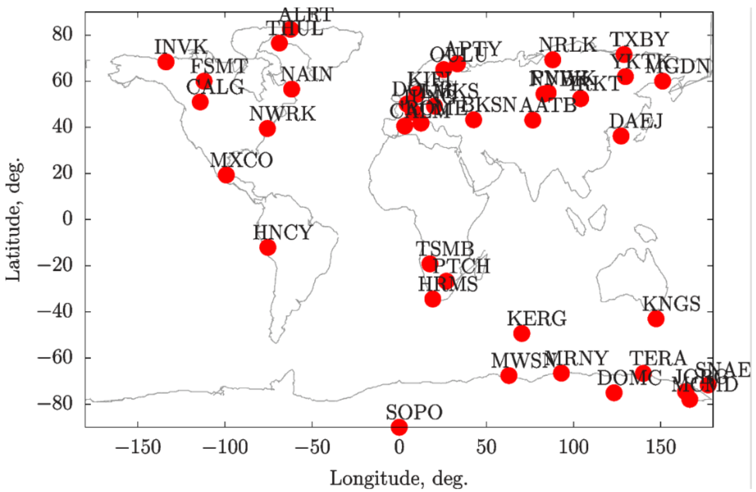

Fig. Distribution of NM station through the Earth

Method of global survey
[A.M. Altukhov, G.F. Krymsky
A.I. Kuzmin, Proc. 11th ICRC, 1969]

$$I^i=\sum_{n=0}^{m}\sum_{m=0}^{\infty}(a_n^m x_n^{m,i}+b_n^m y_n^{m,i})K_n^i$$

$$K_n^i=\frac{\int_{E_{min}}^{\infty}W^i(E)f_n(E)dE}{\int_{E_{min}}^{\infty}W^0(E)f_n(E)dE}$$

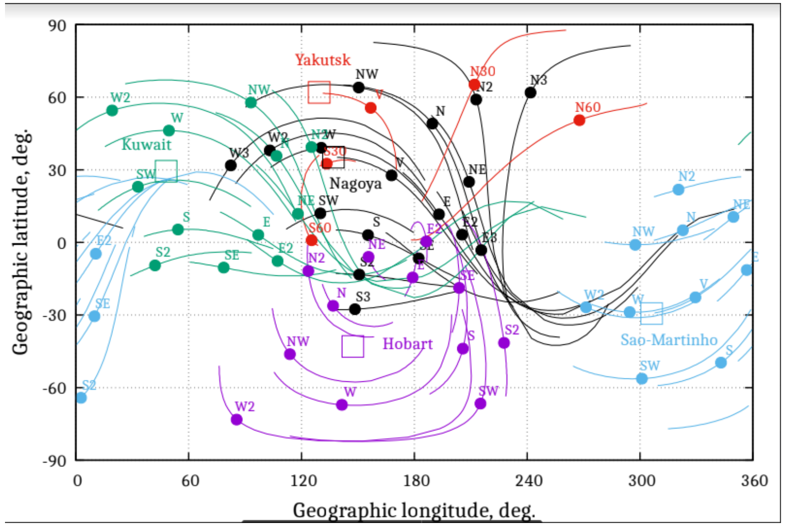

Fig. Asymptotic angles of particle arrival for the GMDN and Yakutsk MT. Solid curves are particle arrival points at different energies from 20 to 1000 GeV. The symbols indicate the asymptotic angles with energies *E med* . [Gololobov et al., Astropart. Phys., 2021]

2. Metodology of treatment of data of ground-based CR detectors

Method of «effective energies» for estimation the absolute flux and energy spectrum of SCR based on NM data [Krymsky et al., JETP Lett., 2008]

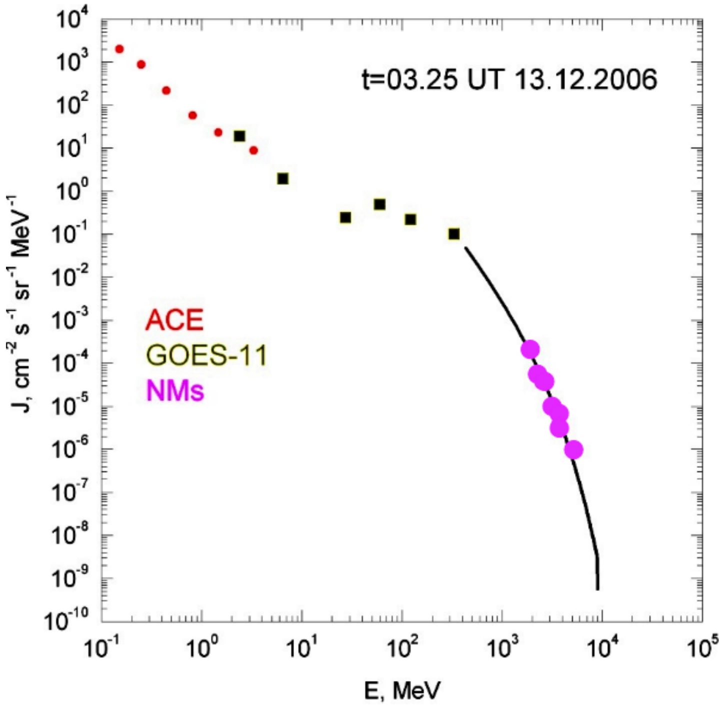

Fig. Energy spectra obtained by the data of NMs (open points), ACE and GOES-11 spacecrafts and by the method [Vashenyuk et al., Geomag. Aeron., 2008].

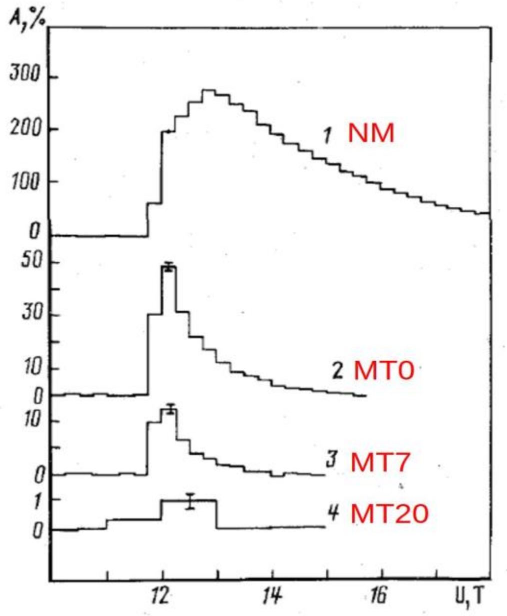

Fig. The event on 29 September 1989 registered by NM and underground meson telescopes of Yakutsk spectrograph [Krymsky et al., DAN, 1990]

Prospects of future development:

1. Continue observation of CR by the spectrograph;
2. Involving the new scintillation muon telescope SMT into the investigations;
3. Improve the global survey method based by simultaneous using both NMs and MTs. Adding the other detectors for better resolution.
4. Development of the methodology of "effective energies" by addition MT data, for investigation the upper limiting energy of SCR.

3. Results of investigation of various aspects of CR heliospheric modulation performing in ShICRA SB RAS :

3.1. Basic model of heliospheric modulation

Basic model of CR heliospheric modulation [Krymsky, JETP, 2007]

Explains CRs behavior in the energy range 100 MeV up to 100 GeV!

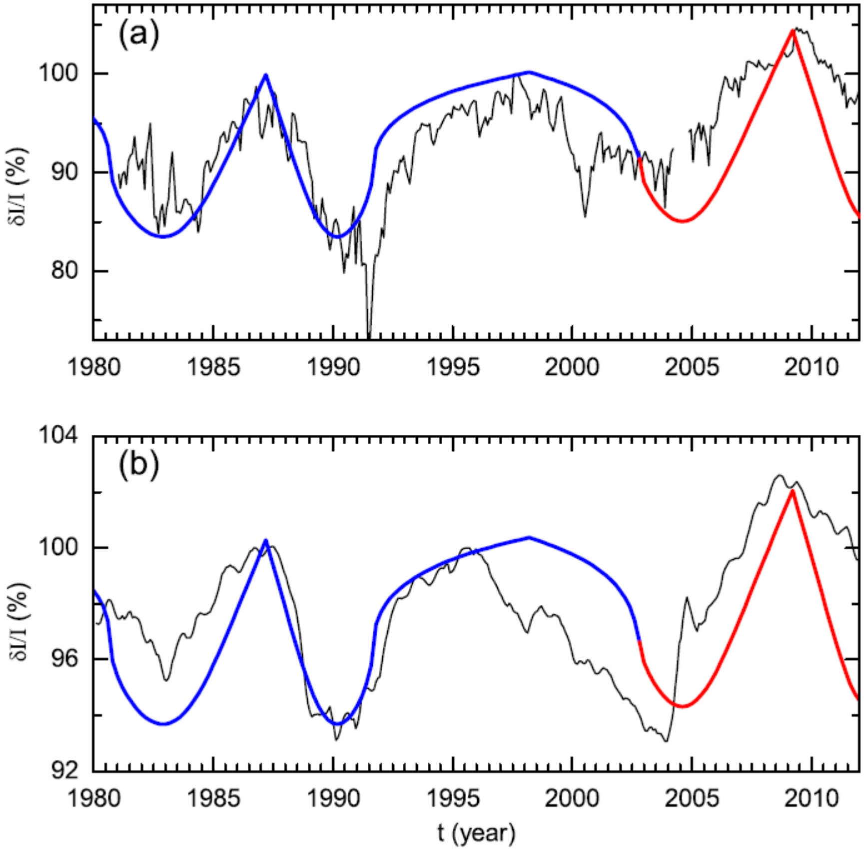

Fig. CR intensity $\delta I/I$ recorded by Yakutsk NM and MT. Red curve – k_0=5 blue curve is for k_0=15. [Gerasimova et al., PoS, 2013]

Based on **4 main modulation processes:**

- **Convection** caused by SW expansion;
- **Diffusion** (particle scattering by turbulent IMF)
- Energy changes such as **adiabatic losses** of energy and acceleration;
- **Drift** caused by the IMF gradient and curvature

The only free parameter:

$$\boxed{k = \frac{H_0}{H_t}} \qquad k = \frac{\sqrt{1-\phi^2}}{\phi + \frac{1}{k_0}}, 0 < k < k_0, 0 < \phi < 1$$

H_0 - regular MF strenght
H_t - turbulent MF strenght

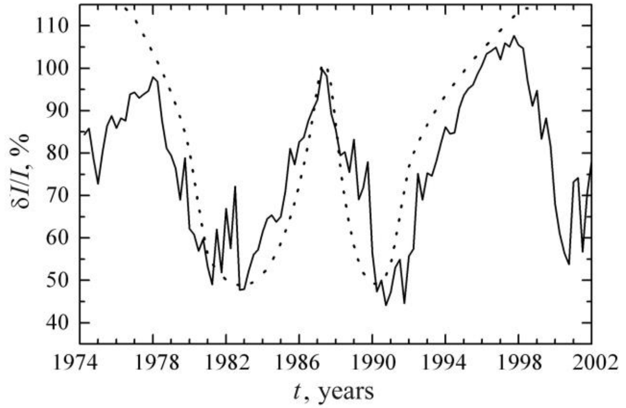

Fig. CR intensity $\delta I/I$ recorded by IMP-8 spacecraft in the channel 145–440 MeV. Dashed curve is for k_0=5. [Gerasimova et al., JSTP, 2017]

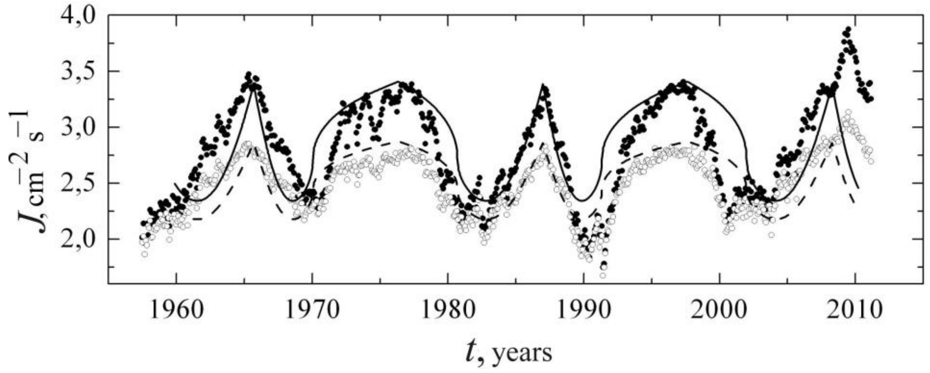

Fig. CR fluxes by measurements in the Stratosphere over Murmansk (closed points) and Moscow (open points). Solid and dashed curves are results of calculation for k_0=5. [Gerasimova et al., JSTP, 2017]

3.2. Theory of acceleration of SCR in front of shock wave

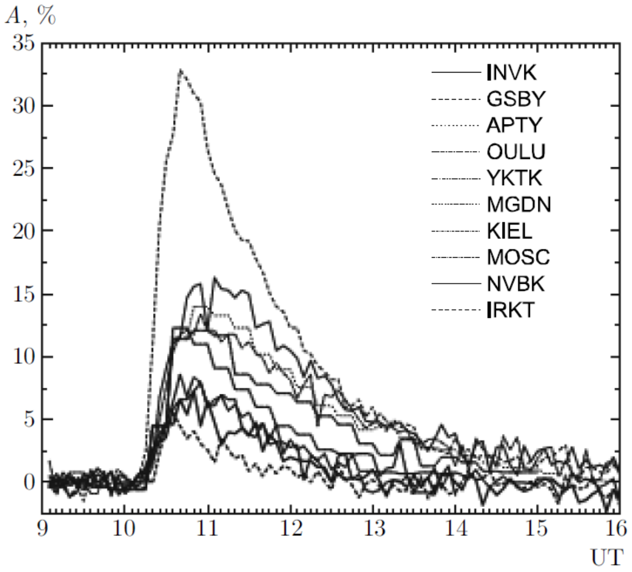

Fig. GLE #30 in 22nd November of 1977 recorded by the global network of NMs [Taneev et al., JETP, 2019].

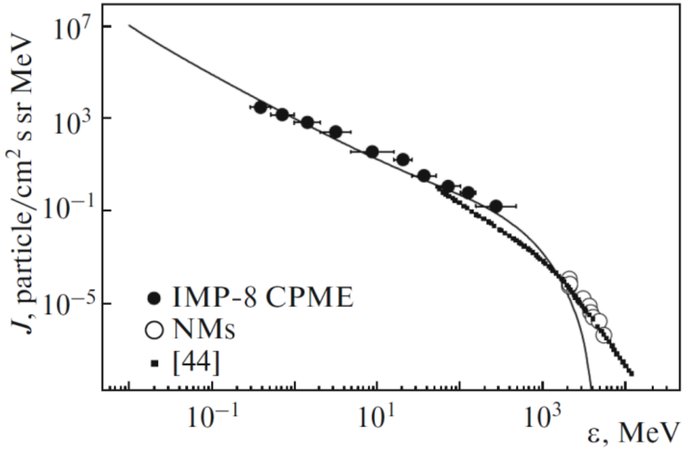

Fig. Comparison of the observed and calculated SCR spectra in the Earth's orbit in the November 22, 1977 event. [Taneev et al., JETP, 2019].

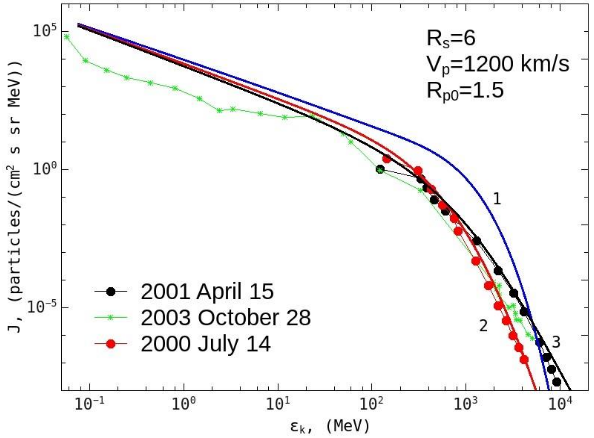

Figure. Comparison of the theory calculation vs the different parameters of the turbulence. Points denotes experimental measurements. Line 1 – the Kolmogorov power law index of turbulence 5/3, Line 2 – 2.2, Line 3 – 2.4. [Petukhova et al., 2017]

Mechanism of regular acceleration of charged particles in shock wave front
[Krymsky, DAN, 1977] *(in Russian)*

[Berezhko, Petukhov, Taneev, 1998]
[Berezhko, Taneev, Astr. Lett., 2003]
[Berezhko, Taneev, Astr. Lett., 2013]
[Petukhova et al., ApJ, 2017]
[Taneev et al., JETP, 2019]
[Taneev, Berezhko, JETP, 2020]

The results obtained do not solve the problem of the origin of SCRs in gradual events, since theoretical works use a free parameter - the coefficient of spatial diffusion of particles in the solar atmosphere. In order to solve the problem, it is planned to solve the following tasks:

1. Injection into interplanetary space of relativistic SCRs accelerated by a shock wave.
2. Self-consistent acceleration of particles and generation of Alfvén waves during acceleration by a shock wave.
3. Elemental (chemical) composition of SCR in gradual events.
4. To compare the results of calculations and measurements in interplanetary space, investigate the SCR propagation taking into account the effect of the accompanying CME.

3.3. Formation of FD in magnetic clouds

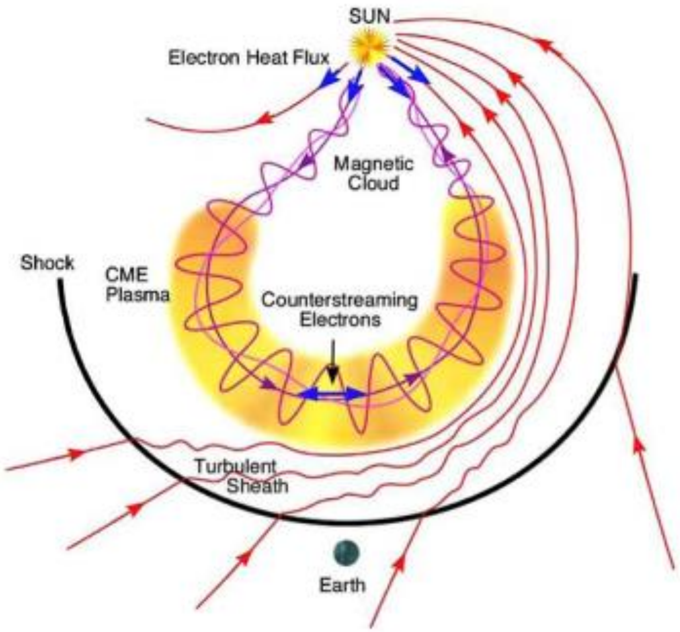

Fig. Schematic illustration of propagation of solar wind disturbance into the interplanetary medium [Zurbuchen, Richardson, Space Sci. Rev., 2006]

Theory of formation of FD in a magnetic cloud (MC)

Electromagnetic mechanism for the formation of a FD in a MC, in which the CR distribution function is determined by energy losses in an inductive electric field and quasi-trapping in a helical magnetic field.

[Petukhov, Petukhov, Bull. RAS, 2013]
[Petukhova,Petukhov, Petukhov, JETP Lett., 2015]
[Petukhova et al., Bull. RAS, 2017]
[Petukhova et al., JGR, 2019]
[Petukhova et al., Ap J., 2019]
[Petukhova et al., Space Weather, 2020]

MC defined by [Miller & Turner., Physics of Fluids, 1981]

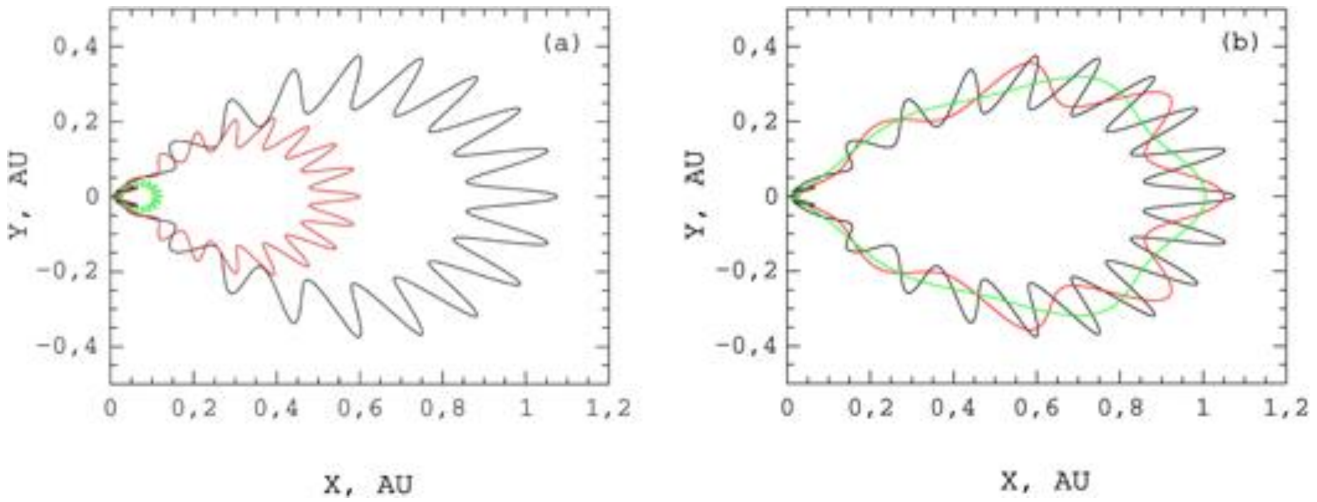

Figure 2. Projection of magnetic field lines on the *X0Y* plane. (a) One magnetic field line for three time moments. (b) Three magnetic field lines located at different distances from the MC surface for one time moment. [Petukhova et al., Ap J., 2019]

3.3. Formation of FD in magnetic clouds

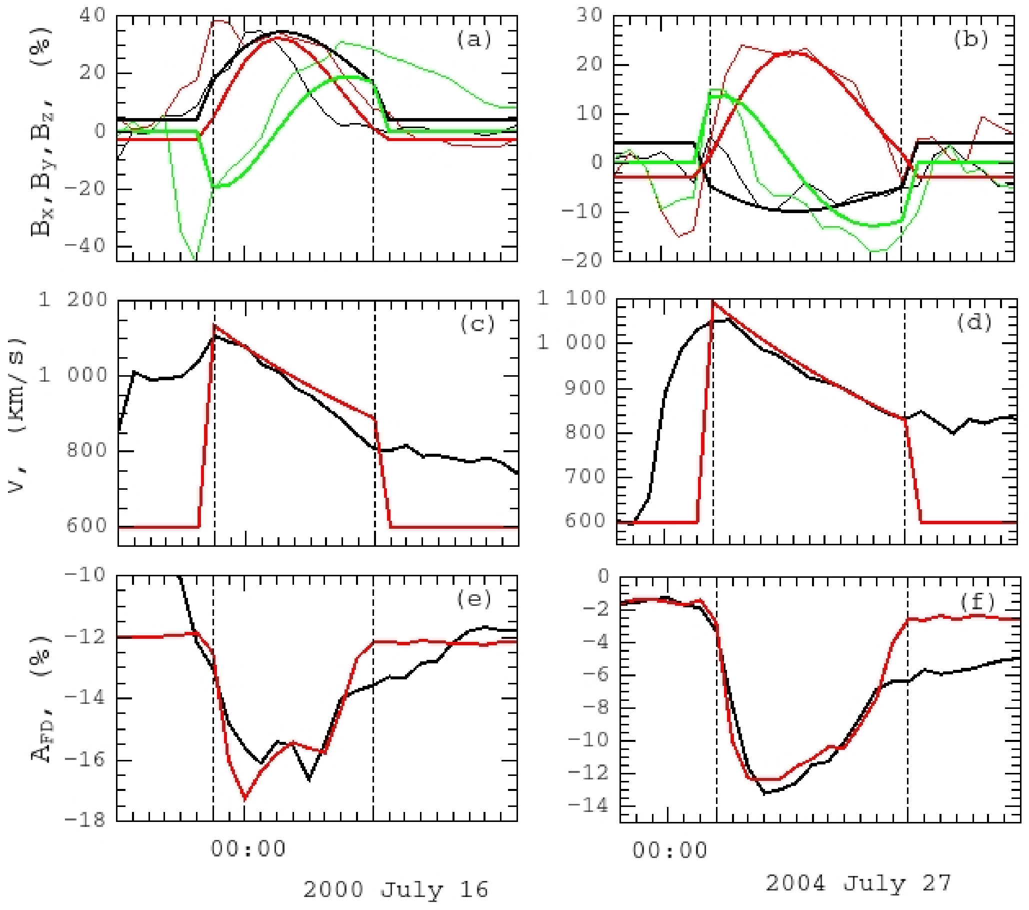

Figure (a, b) Magnetic field components in UT. The black, red, and green lines correspond to Bx , By , and Bz components of the magnetic field. Thin lines are measurements; thick ones of the corresponding color are model calculations. (c, d) Plasma velocity. (e, f) The FD amplitude. In the panels (c–f), black lines are measurements; red lines are calculations. The interval between minor ticks is 1 hr; the major tick is the beginning of the day. The vertical dashed lines are the MC boundaries. [Petukhova et al., Space Weather, 2020]

the main moments of the model:

- The model does not have any free parameters. The structure of the MC and its propagation geometry are determined from the data of direct measurements by spacecraft;
- Comparison of model calculations with experimental data shows good agreement;
- The model can be used to describe the second step of FD:

The calculation shows that characteristics of FD in MC depends on:

1) IMF strenght, MF’s structure and its statements in the volume, the solar wind’s speed and gradient;
2) Angular size and the MC cross sectional area;
3) Trajectory of MC crossing by the Earth;

In continuation of studies of the formation of FD, it is planned to:

1) Study of the relationship between the helical structure of the magnetic field in the entire volume of the MC and the amplitude of FD for low energy CRs.
2) The contribution of alpha particle on the FD spectrum in MC.
3) Comparison of the results of modeling and measurements on a large number of events.
4) Development of a FD model that takes into account the combined action of the diffusion mechanism in sheath region of ICME and the electromagnetic mechanism in the MC.

3.4. Structure of the heliosphere.
North-south asymmetry (NSA) of the heliosphere.

First signature on existence if NSA of the heliosphere:
- Heliolatitudinal distribution of SCR events arriving to Earth [Krymsky et al., 1964] *(in Russian)*
- Annual variations of CR intensity [Krymsky et al., 1981] *(in Russian)*

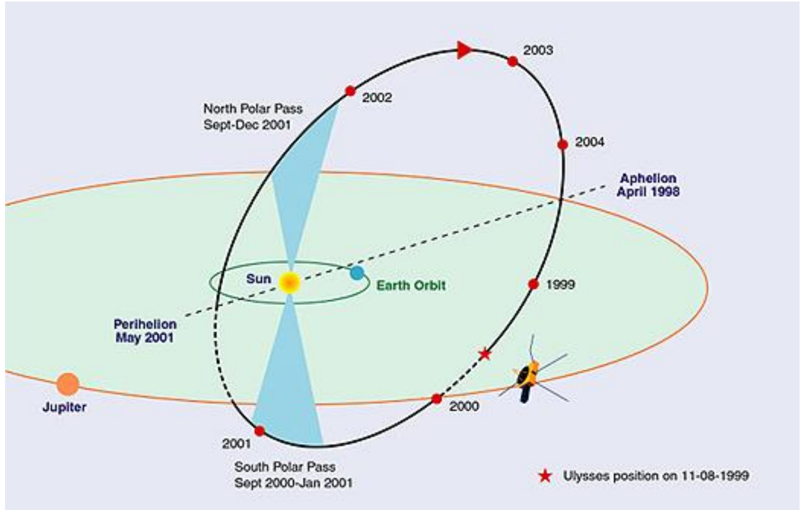

Fig. Trajectory of 2nd Fast Latitude Scan of Ulysses spacecraft https://science.nasa.gov/science-news/science-at-nasa/2004/17mar_ulysses

Convincing evidence of NSA [Simpson et al., 1996]
Ulysses made Fast Latitude Scans of the Sun in 1994-1995, 2000-2001, and 2007-2008.

Fig. Heliolatitude distribution of CRs on the Ulysses spacecraft relative to the IMP 8 data. red lines represent the distribution expected in model. [Krymsky et al., Astr. Lett., 2009] <u>$\approx 7^\circ$ **shifted to the south of solar equator**</u>

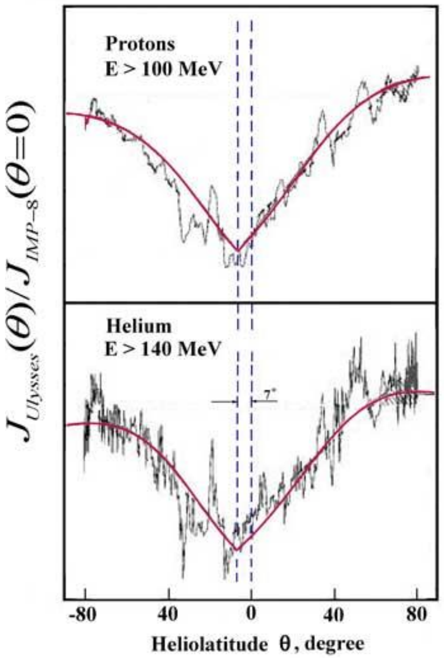

- CR anisotropy obtained by Yakutsk MTs revealed dependence on heliolatitude [Krymsky et al., 2006]
- Relation between NMs intensity dependence to the form of HCS [Krymsky et al., JETP, 2007]
- CR anisotropy and intensity during crossings of HCS revealed NSA [Krymsky et al., JETP Lett., 2012]
- NSA revealed itself in TA data, <u>**showing a $\approx 4-5^\circ$ shift**</u> to the south [Krymsky et al., 2014]

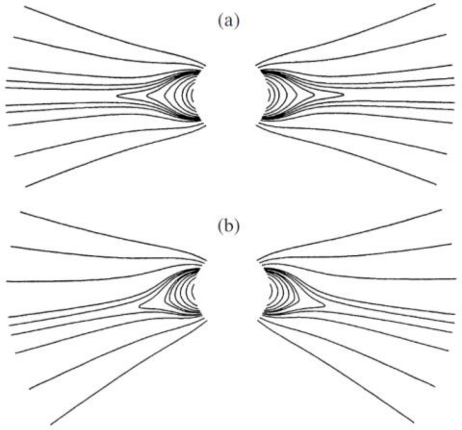

Fig. Magnetic field lines near the Sun for symmetric(a) and asymmetric (b) magnetic fluxes. [Krymsky et al., Astr. Lett., 2009]

<u>Future plans:</u>
Since the Ulysses spacecraft finished operating (2009) and there is no any like missions at the current moment, the role of CRs in investigation of NSA is significantly increased.
The NSA should be re-estimated for 23-24 solar cycles.

3.5. CR tensor anisotropy

Tensor (bi-directional) **anisotropy** of CR or second spherical harmonics

Possible explanation - CR screening by sectors of the interplanetary magnetic field [Krivoshapkin et al., Proc. 11th ICRC, 1970]

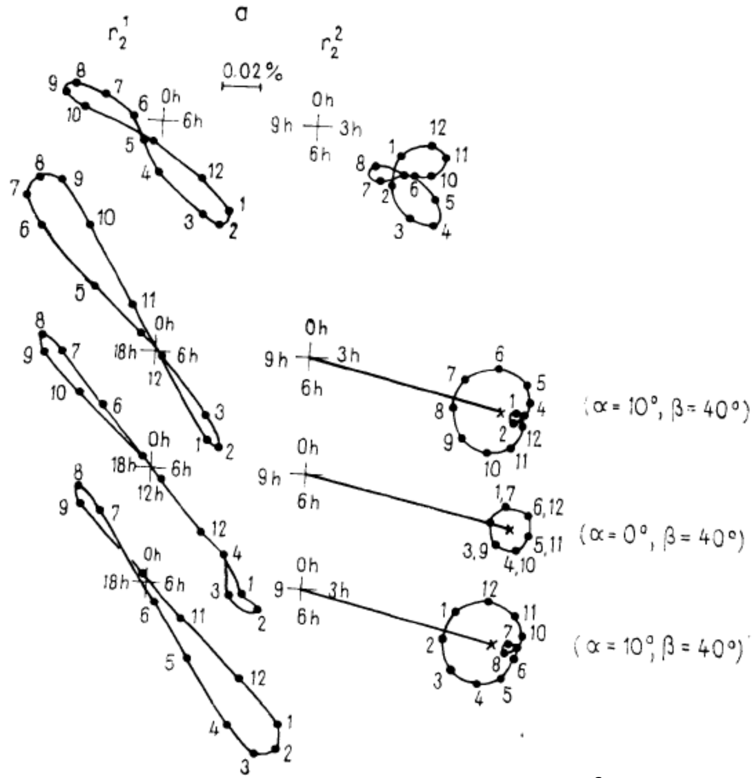

Pic. Tensor anisotropy components in free space obtained by data of the world network of NM stations for 1959, 1964, 1965. [Krivoshapkin et al., Proc. 11th ICRC, 1969].

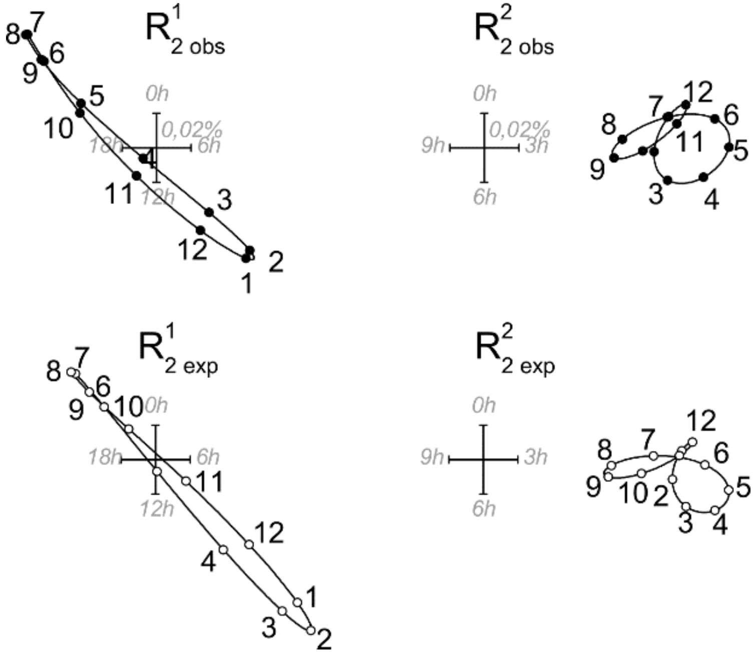

Pic. Diagram of yearly change of the components ($R^1_{2,obs}$ and $R^2_{2,obs}$) of CR tensor anisotropy obtained using Nagoya MT for 1971-2017. $R^1_{2,exp}$ and $R^2_{2,exp}$ are results of modeling [Gololobov et al., JPCS, 2019].

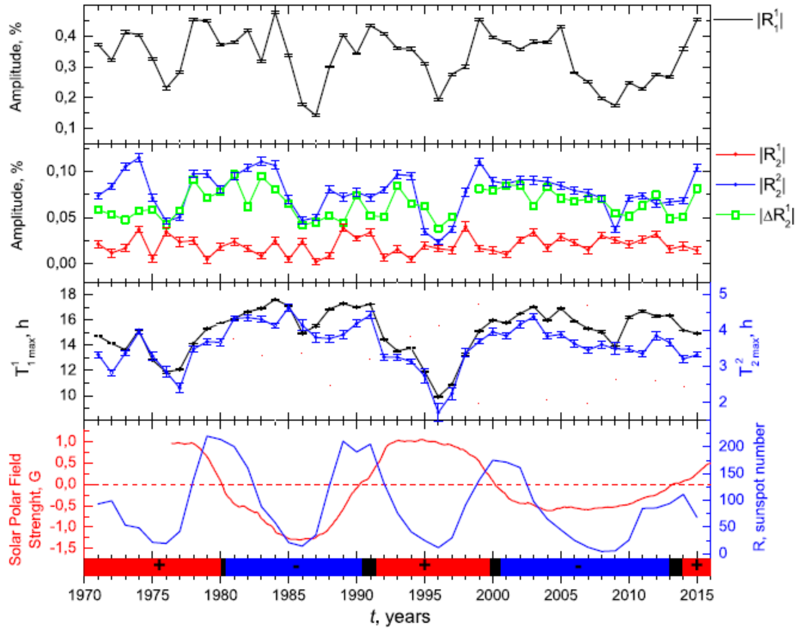

Pic. Vector diagram of yearly change of the components ($R^1_{2,obs}$ and $R^2_{2,obs}$) of CR tensor anisotropy obtained using Nagoya MT for 1971-2017. $R^1_{2,exp}$ and $R^2_{2,exp}$ are results of modeling [Gololobov et al., PoS, 2017].

Conclusions

We’ve presented a brief information on:

- modern statement of Yakutsk CR spectrograph after A.I. Kuzmin;
- methods of treatment of data of ground-based CR detectors performed in ShICRA.

In near future we plan to continue the investigations in the following directions:

1. 11-year variations of CR intensity;
2. Forbush Decreases;
3. SEP(SCR);
4. The structure of the heliosphere (north-south asymmetry);
5. Tensor anisotropy of CRs;